A centrifuge for studies of fluid dynamics phenomena in a rotating frame of reference

M. Vargas
† *Instituto Tecnológico de Zacatepec*
A.P. 45, 62780, Zacatepec, Mor., México.

E. Ramos
‡ *Centro de Investigación en Energía*
Universidad Nacional Autonoma de México
A.P. 34, 62580, Temixco, Mor., México

G. Ascanio
Centro de Ciencias Aplicadas y Desarrollo Tecnológico
Universidad Nacional Autonoma de México
A.P. 70-186, 04510, México, D.F., México.

R. Espejel
Instituto de Física UNAM
A.P. 20-364, 04510, México, D.F., México.

G. Esquivel† and G. Hernández-Cruz‡

Recibido el 13 de junio de 2001; aceptado el 11 de febrero de 2002

A centrifuge for the study of fluid mechanics phenomena in a rotating frame has been constructed at the Center for Energy Research at the National University of Mexico (UNAM). The centrifuge has a 1.5 m long arm and is designed to rotate at a maximum rate of 86 rpm which corresponds to a maximum centrifugal acceleration of 13 g. This paper describes the mechanical characteristics of the centrifuge and its instrumentation. The potential of the system for performing fluid mechanics experiments in a rotating frame of reference is also discussed and sample results of natural convection in a cavity are presented.

Keywords: Centrifuge; fluid dynamics; microgravity; natural convection; Coriolis force

Se construyó una centrífuga para el estudio de fenómenos de la dinámica de fluidos en un marco de referencia rotatorio. La centrífuga tiene un brazo de giro de 1.5 m de longitud y se diseño para rotar a una tasa máxima de 86 rpm, la cual corresponde a una aceleración de 13 g. Este artículo describe las características mecánicas de la centrífuga y su instrumentación. Se muestra el potencial del sistema en el desarrollo de experimentos de mecánica de fluidos en un marco de referencia rotatorio y se presentan algunos resultados de la visualización de la convección natural en una cavidad.

Descriptores: Centrífuga; dinámica de fluidos; microgravedad; convección natural; fuerza de Coriolis.

PACS: 01.52.+r; 47.27.Te; 47.32.-y

1. Introduction

Centrifuges have been used to explore a large variety of physical phenomena with augmented gravity, ranging from the study of statics and failure of materials used in civil engineering to the determination of human response to time dependent supergravity. A specific application of centrifugation that has an enormous potential for applications in microelectronics, solar energy, and other fields is crystal growth. The improvement of the quality of the semiconductor crystals is the ever present goal of material science researchers and manufacturers. With this aim in mind, some sophisticated experiments were performed in the MIR station and German sounding rocket TEXUS 24 some years ago. The main objective was to clarify the role played by the buoyancy force that generates the convective motion in a crucible in the quality of crystal. Buoyancy is the force which is exerted on a fluid due to variations of density and in the presence of a gravitational field. Fluid parcels with lower density move in a direction opposite to that of the body force and fluid parcels with higher density move in the same direction as that of the body force. It has been found that the absence of the force of gravity increases the crystal homogeneity when crystals are grown in crucibles, for example with the Czochralski method. However, because of their enormous costs, the extraterrestrial methods for crystal growth are impractical. In a further effort to explore the effect of body forces on the crystal growth process and as an alternative approach, crystals were grown in centrifuges. Furnaces were mounted in centrifuges and rotated to obtain centrifugal accelerations of up to 50 g (g is the terrestrial acceleration constant; 9.81 m/s^2). The results of these experiments were successful in the sense that specific values of the rotation rate yielded enhanced crystal quality. However, considerable difficulties have been encountered by many mate-

rial scientists around the world to use centrifuges to perform crystal growth experiments since most centrifuges were constructed for other purposes. The centrifuge used by the Soviet team lead by L. Regel to perform crystal growth experiments was a $18\ m$ arm with a rotation velocity at $36.5\ rpm$ machine at Star City near Moscow. This centrifuge was used to train cosmonauts to withstand high accelerations during take off and reentry of spacecrafts. The results of these pioneering work has been described by Burdin *et al.* [1]. The $5.5\ m$ maximum arm centrifuge used by Rodot *et al*. [2] to perform crystal growth experiment at Nantes in France belongs to the Department of Roads and Bridges and is used mainly for civil engineering studies on small scale models. Another relevant centrifuge used occasionally for materials processing, is the C CORE (Centre for Cold Ocean Resources Engineering) which is located on the campus of Memorial University of Newfoundland, Canada. Its principal use is geotechnical research. This Acutronics $680-2$ is capable of generating up to $200\ g$, and has a $5\ m$ nominal radius, its maximum rotational speed being about $189\ rpm$ see Ref. 3. At the Tsukuba Space Center, the National Space Development Agency of Japan (NASDA) built a centrifuge with 7.25 *m* arm, which reaches up to $10\ g$ with an angular velocity of $35\ rpm$. This device was used to reproduce several of the German rocket TEXUS 24 experiments as described by Hibiya *et al*. [4].

A centrifuge constructed specially for materials processing research and related flow visualization, is the HIRB (High Inertial Rotating Behemoth) at the International Center for Gravity Materials Science and Applications in Clarkson University. It has a $1.5\ m$ arm, with a maximum attainable rotation rate of 90 *rpm* and a maximum acceleration of $13.8\ g$. A complete description of this instrument is given by Deribail *et al*. [5]. The Erlangen University group constructed a centrifuge in 1980, with a $0.75\ m$ arm and velocity range of 12–$250\ rpm$, capable of generate up to $50\ g$. Subsequently, the centrifuge design was modified to incorporate two arms, one of $2.6\ m$ and an other of $1.6\ m$. This centrifuge was used to test the effects of Coriolis and centrifugal forces in several crystal growing experiments. Some of the results are reported in Refs. 6 - 8. Many experiments were done in these centrifuges for the development of new materials like high-quality semiconductors for the microelectronics industry. An important source of information on the progress of understanding the physics of the phenomena occuring in rotating systems in the context of materials research is the series of books that contain the proceedings of the Clarkson conferences on centrifugal phenomena. [9, 10, 11].

In this paper we present the design and details of the construction of a centrifuge. Also we describe sample results obtained with this device. It is important to remark that in contrast with other centrifuges, this equipment was designed and constructed with the principal objective of studying the effects of centrifugal and Coriolis forces in fluid dynamics phenomena.

2. Definition and design criteria

The long-term objective of the project which encomposses the design and construction of the centrifuge, is the study of several physical phenomena that occur in a non-inertial frame as seen from the laboratory frame of reference. Of particular interest is the effect of virtual forces on the motion of nonisothermal flows. For this reason, one important design criterium is the modularity and flexibility to allow modifications or changes in the relative position of the components. In the two following subsections, we present the design criteria of the centrifuge, emphasizing the features that are required for the study of natural convection in cavities where a temperature difference is imposed. In this spirit, we will restrict the discussion to the study of flows in closed cavities where a temperature difference is imposed externally. The physical phenomena that occur in the centrifuge are modified by the presence of the centrifugal and Coriolis forces. The centrifugal force is a conservative force and has the form

$$F_{cent} = -\frac{\rho}{2}\nabla \left|\omega \times \mathbf{r}\right|^2 ,$$

where ρ is the density, $\mathbf{r}$ is the distance from the rotation vector, and ω is the angular velocity. The Coriolis force is defined by the expression

$$F_{Coriolis} = 2\omega \times \mathbf{u},$$

where $\mathbf{u}$ is the local velocity. From its definition, it is seen that the Coriolis force occurs only if the system is in motion and therefore, has an influence only under dynamic conditions.

2.1. Geometrical considerations

The phenomenon of natural convection in a rotating frame of reference depends fundamentally on the relative orientation and position of three vectors. First, there is unavoidable gravity acceleration vector, then the rotation vector, and finally the temperature gradient vector, which indicates the direction of the temperature difference imposed on the cavity. Ideally, we are interested in a situation in which the rotation vector is perpendicular to the temperature gradient vector, in such a way that the centrifugal force can be oriented along the axis of the cavity and parallel to the temperature gradient vector. This situation is illustrated in Fig. 1 for a natural convective cavity composed of a cylindrical container, where the plane walls are held at constant but different temperatures. In the absence of terrestrial gravity, this arrangement would lead to a simple situation where essentially the only new effect would be that of the Coriolis force. Although the generation of these physical conditions is not possible due to the ever present gravity force, the following very convenient arrangement can approximate these conditions: at the end of the arm of the centrifuge, a container that houses the experimental equipment is attached by a hinge that allows rotation around a horizontal axis. When the centrifuge is set in motion, the container aligns itself with the vector sum of the centrifugal and gravity forces, as shown in Fig. 2. Under these conditions the sum of conservative forces is parallel to the temperature gradient vector.

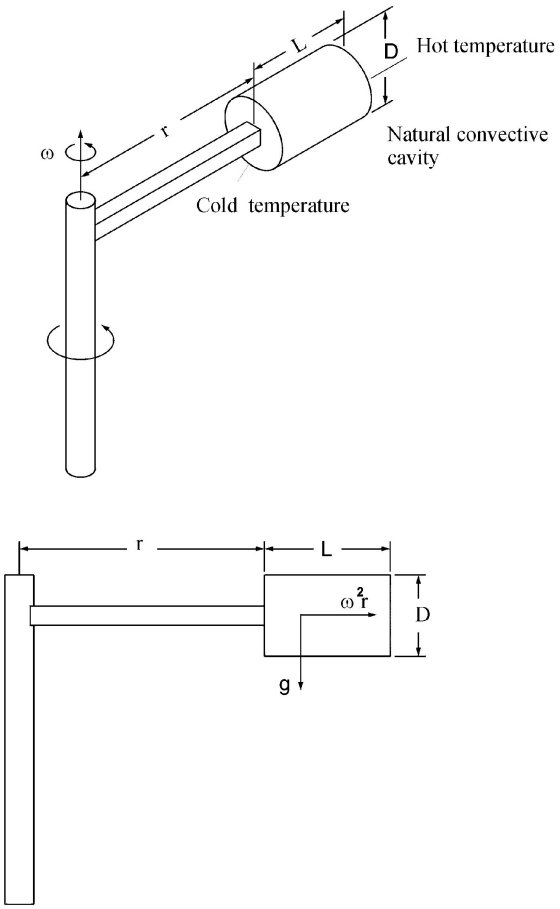

FIGURE 1. Ideal set up for testing the influence of Coriolis force in a natural convective cavity.

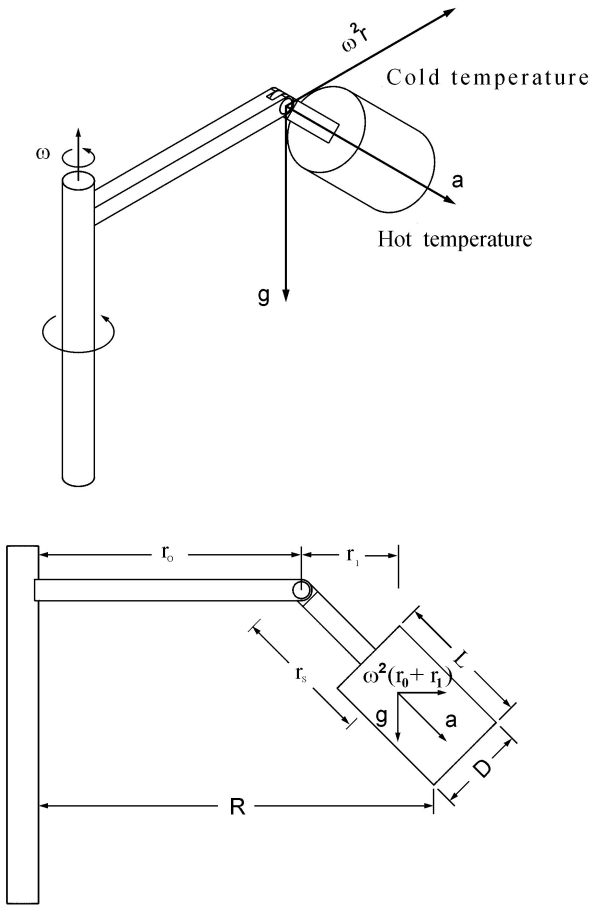

FIGURE 2. Realistic arrangement for observing the influence of Coriolis force in a centrifuge.

2.2. Physical considerations

The most basic information required for the design of the centrifuge are the ranges of the nondimensional parameters of relevance in the natural convective flows. As is well established, the qualitative properties of natural convective flow are described by two parameters: the Prandtl and Rayleigh numbers [12]. The Prandtl number is the ratio of kinematic viscosity ν to thermal diffusivity α (*i.e.* $Pr = \nu/\alpha$). Therefore, it indicates the ability of a material to transfer momentum as compared to its ability to transfer heat. We are interested in studying natural convection of liquid metals, air, water and Silicon oils, covering a range of Prandtl number from 10^{-2} to 10^2. This requirement does not impose technical difficulties except for visualization. In the present design we restrict ourselves to transparent materials. The Rayleigh number Ra is defined by

$$Ra = g\beta\Delta T L^3/\alpha\nu,$$

where β is the volumetric expansion coefficient, L is a characteristic length of the cavity and ΔT is the temperature difference.

It is recognized now that the nonrotating natural convection in cavities exhibits essentially three different qualitative behaviors:

a) nonconvective regime, where the velocity is zero and heat is transferred solely by conduction,

b) steady state convection where the flow is laminar, and

c) unsteady regime that includes chaotic and turbulent regimes.

Figure 3 shows a Ra vs aspect ratio ($\Gamma = L/D$) map indicating the regions where different qualitative flows occur, for the particular case of a cylindrical container with circular cross section and $Pr = 6.7$. Our interest is to design a device such that it allows us to observe the influence of rotation on all three (nonrotating) regimes. In a rotational flow, several nondimensional numbers have been defined [13]. In the context of the centrifuge project, the most relevant one is the Taylor number defined by

$$Ta = 4\omega^2 L^4/\nu^2.$$

This nondimensional parameter relates the effects of Coriolis and viscous forces, a vanishing Taylor number indicates no rotation. Qualitative modifications of natural convective patterns have been observed to occur for a fluid with $Pr = 0.13$ at a Rayleigh number of 10^5, [7].

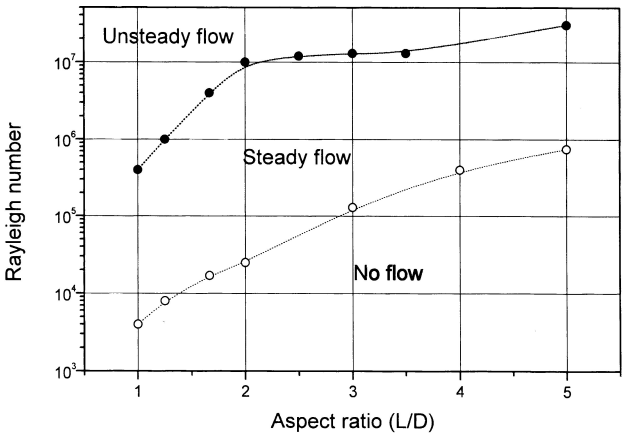

FIGURE 3. Rayleigh number versus aspect ratio map of qualitative dynamic behavior for a cylindrical container with $Pr = 6.7$. Adapted from Ref. 14.

De la Cruz [13] found that the Taylor number required to supress oscillatory flows for a $Pr = 5$ fluid at a $Ra = 4\times10^5$ was $Ta = 5 \times 10^6$. In principle, it would be convenient to build a centrifuge capable of rotating at large enough rates to explore the reported modifications in the qualitative behavior of the natural convective flow. Therefore we established the range $0 < Ta < 10^8$ for working fluids with $\nu = 3.0 \times 10^{-5}\ m^2s^{-1}$ as a minimum design requirement for the centrifuge, given that the visualization equipment of the convective cavities imposes a minimum height of about $0.02\ m$. The rotation rate required to reach the desired ranges of Taylor numbers for the smaller cavity is approximately 80 rpm. The Ekman number is alternative notation for the Taylor number and is defined by Ek=$\nu/2\omega L^2$. Another nondimensional parameter is the Rossby number $Ro = U/2\Omega L$, where U is the local velocity of the system, L is the characteristic length and Ω is the rotational velocity. This number is the ratio between inertial and Coriolis forces. If $Ro \gg 1$, the influence of rotation is small. In the other case, when $Ro \ll 1$ the rotation motion determines the flow regime and its patterns. Boubnov and Golitsyn [12]. It would be desirable to predict the characteristic velocity of the flow. A tempting idea would be the use of the so-called free fall velocity which arises from the balance between inertial and buoyancy effects,

$$u = (g\beta\ \Delta T\ L)^{1/2}.$$

This expression however overestimates the velocity by a factor that depends on the aspect ratio of the container, since it does not take into account the influence of the walls. Experimental observations indicate that for aspect ratios of $L/D \backsim 2$, and water as test fluid, the vertical velocity approaches is of order $u \sim 4 \times 10^{-4} ms^{-1}$.

Once the ranges of the variables presented in the previous paragraphs have been established, it is possible to determine the ranges of nondimensional parameters that describe the physical effects present in the system. Table I gives definitions and involved of nondimensional parameters including the ranges of these parameters that can be achieved with the centrifuge.

TABLE I. Main nondimensional parameters

Prandtl Pr	ν/α	10^{-2}-10^2
Rayleigh Ra	g$\beta\Delta TL^3/\nu\alpha$	10^5-10^7
Taylor Ta	$4\omega^2L^4/\nu^2$	0-10^9
Eckman Ek	$\nu/2\omega L^2$	3×10^{-5}-∞
Rossby* Ro	$U/2\omega L$	10^{-4}
Reynolds* Re	UL/ν	10^{-1}-30
Froude Fr	$(\omega^2L/g).(H/L)$	0 - 10^{-1}
Rotational Rayleigh Ra_r	$a\beta\Delta TL^3/\nu\alpha$	10^5- 10^8

*We used the experimental velocity $U = 4 \times 10^{-4} ms^{-1}$, as the characteristic velocity.

3. Mechanical design and instrumentation

The main components of the centrifuge are the nonrotating components, the rotating structure, two baskets, a bridge, and a security fence. In this section we describe in detail the mechanical properties of these components. Here we also present the equipment housed in the experimental basket which was used to obtain the experimental results given in the last section of this article. The two most relevant features of the rotating system are an arm length of $1.5\ m$ and a maximum angular speed of $\omega = 86\ rpm$ ($9\ rad/s$).

3.1. Nonrotating components

The nonrotating components of the centrifuge are the base, the central support frame, the bearings, the motor, and the transmission system, as displayed in Fig. 4. The centrifuge base is a rectangular steel plate $0.6\ m$ wide, $1.2\ m$ long, and $0.012\ m$ thick, which is fixed to the foundation by six expansion high resistance screws. The motor and the central support frame are anchored to the base. The transmission system is composed of two belts and two pulleys. The rotation of the centrifuge is generated by a $1\ HP$, three phase AC motor capable of developing a maximum torque of $142.35\ Nm$ ($1260\ lb\ plg$) at $1750\ rpm$. Its electrical characteristics are $(208-230)/460\ V$ and $4.2/2.1\ A$ in the stator. The motor velocity control is made by a digital inverter (VS mini C series), with frecuency range of 0 to $400\ Hz$ [16]. The power transmission uses V belt drivers of trapezoidal cross section with efficiency of $70-90\%$ to absorb shocks and operate at low bearing pressure. The transmission system has two aluminium pulleys with a diameter $0.152\ m$ (6"), one of them fixed to the axis of rotation with a double belt. An important feature of the transmission system is the reduction of the mechanical vibrations to a minimum when the centrifuge is in operation.

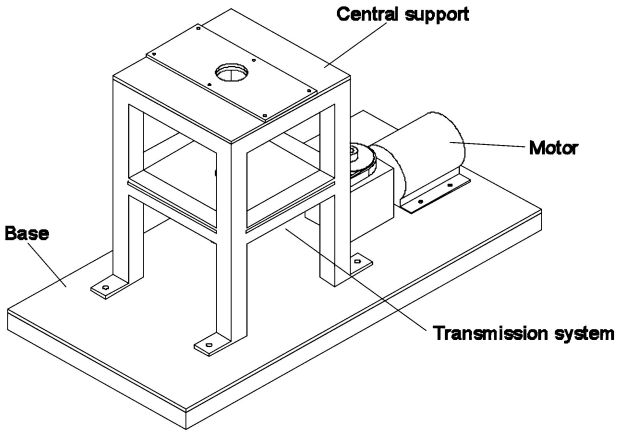

FIGURE 4. Nonrotating elements of the centrifuge. Bearings are under the plates of the central support frame and therefore not shown in the figure. Also the pulleys are hidden by the lower plate of the central support (see Fig. 5).

3.2. Rotating structure and power supply

This arrangement is composed of the shaft, and five modules: one central, two intermediate, and two terminal, as shown in Fig. 5. The shaft is a 4140 steel, $0.101\ m$ (4") diameter and $1.10\ m$ long rod that sits vertically in the central frame held by two bearings of $0.0762\ m$ (3") diameter, and separated a distance of $0.328\ m$. The diameter of the lower extreme of the shaft was reduced to $0.038\ m$ (1.5") to fit the pulleys and the lower bearings. All modules are made of structural carbon steel tubes with a rectangular $0.0254\ m^2$ (1" $\times$ 1") cross section. The intermediate and terminal modules are fixed at opposite sides of the central structure. The central module is a prism $0.4\ m \times 0.4\ m \times 0.6\ m$ that holds the central shaft with two bearings sitting in two steel plates. This module also houses two batteries and the DC/AC inverter. The intermediate modules are trapezoidal prisms; the intermediate ones having large cross sections $0.4\ m \times 0.4\ m$ facing the central module of and a small cross section of $0.4\ m \times 0.14\ m$ in contact with the terminal modules. The length of the intermediate modules is $0.645\ m$. The terminal modules are also trapezoidal prisms, the larger cross section is of $0.4\ m \times 0.14\ m$ and the small cross section is of $0.4\ m \times 0.09\ m$, and their total length is $0.645\ m$. At far end of the terminal modules small steel plates that hold wall bearings are placed. This arrangement supports $0.53\ m$ long stainless steel rods with a diameter of $0.02\ m$ ($9/8$") that constitute shafts that allow horizontal rotation of the swinging baskets located at the end of the arms of the centrifuge. All modules are fixed with high resistance hexagonal head screws. As will be described in more detail below, the maximum total weight of each basket is $10\ kg$, and since the maximum rotation rate is $86\ rpm$ and the arm length is $1.5\ m$, the upper limit of the centrifugal force exerted at the end of the arms is $1215\ N$.

Given the design of the centrifuge and in order to avoid the use of slipping rings, it was deemed necessary to mount on board the rotating section of the centrifuge a power source. This design strategy has the advantage of providing a versatile power supply that can support present and future power demands from the various instruments used in the data acquisition and visualization. The instruments that require electrical power are: the on-board CPU (power consumption $\sim$ $50\ W$), the laser power source used in the visualization system (power consumption $\sim 30\ W$), the thermoelectric devices required for maintaining constant temperature walls (power consumption $\sim 8\ W$), and control circuits (power consumption $\sim$ $2\ W$). Taking into account that of these instruments and allowing for future increases, it was estimated that the total power demand would be $200\ W$.

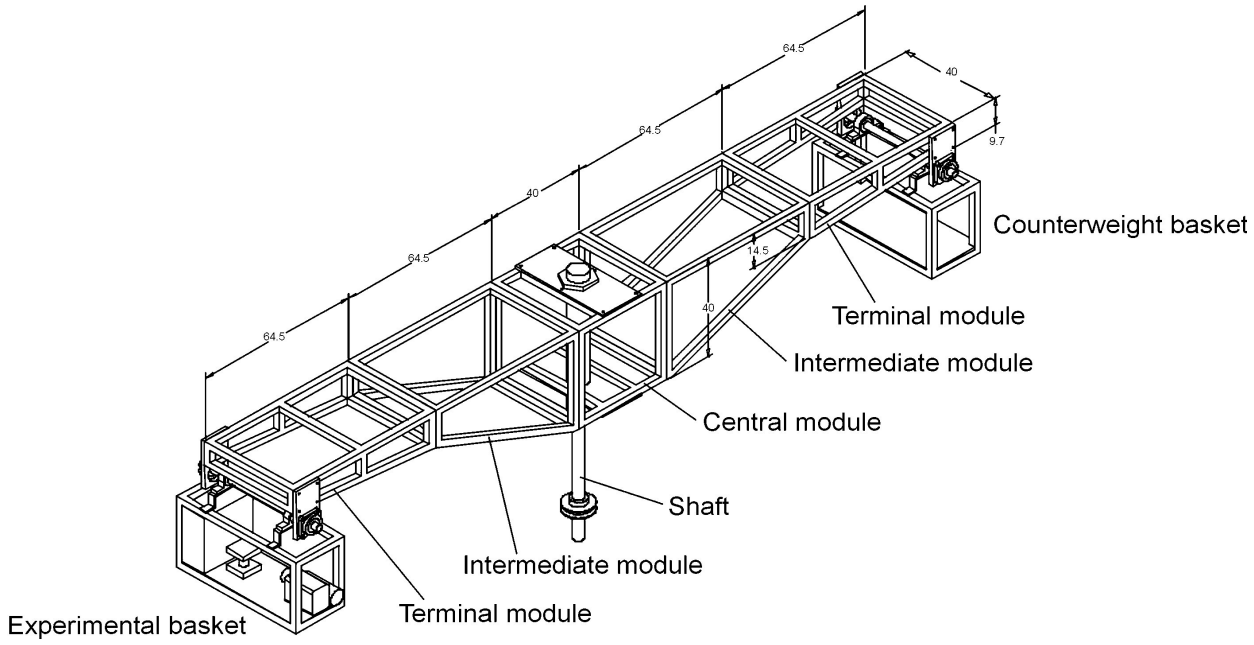

FIGURE 5. Rotating structure of the centrifuge.

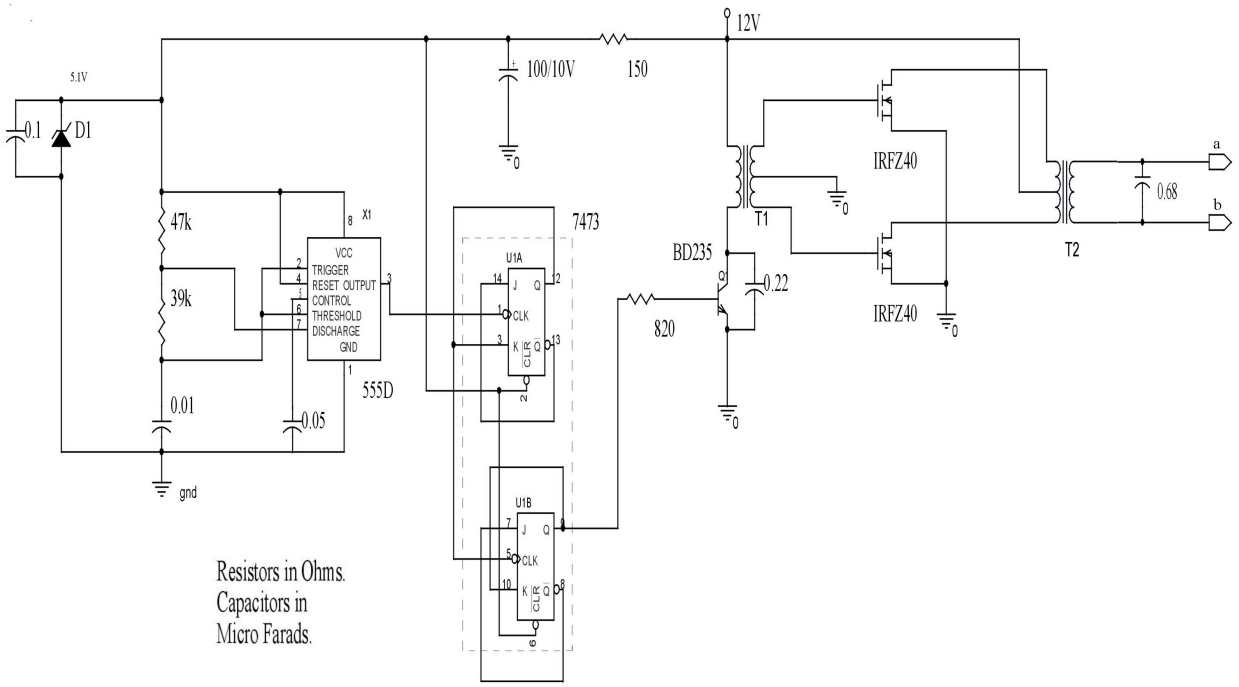

FIGURE 6. Electronic circuit of the DC/AC inverter.

The primary power source is constituted by two $12\ V, 60\ A\ hr$ capacity, lead-acid batteries located near the axis of rotation. With these design parameters and considering an autonomy of 3 hours, the DC/AC inverter was designed. Figure 6 shows the electronic circuit of this device. The alternating system is an RC oscillator composed of the $U2(555)$ integrated circuit, R_1 and R_2 resistors, and C_4 capacitor. These components determine the oscillation frequency. The $U1(7473)$ integrated circuit divides the frequency of the output signal of $U2$ by a factor of four with a duty cycle of 50%. In addition $U1$ controls the bipolar transistor Q_1 coupled in a common emitter configuration with the primary coil of transformer T_1. This device and capacitor C_1 are the resonant load of the collector circuit. This array yields two signals with opposite phase and a long enough time delay to prevent the simultaneous conduction in the $M_1$and M_2 $MOSFET$ transistors. These devices are used as power amplifiers together with the T_2 transformer which increases the voltage to $125\ Vac$. C_5 smoothens the waveform of the output voltage.

There are two important features of the design of this DC/AC inverter that should be emphasized. In contrast with the voltage signal provided by the AC line which is a 125 V_{rms}, sine wave with a frequency of $60\ Hz$, the signal provided by the DC/AC inverter is a 160 V_{rms} square wave at $240\ Hz$. The wave form was choosen to let the power transistors work in a cut-and-saturation mode to minimize dissipation. Also the voltage and frequency have been tailored to the capacitive input of the CPU power supply to further enhance the power conversion and transfer.

3.3. Experimental and counterweight baskets

At the end of the arms of the centrifuge two rectangular baskets were set, one of them is the experimental and the other is the counterweight basket. When the centrifuge rotates, the position of the baskets will have a tilt due to the simultaneous action of the centrifugal and the gravity forces. The baskets are constructed with DEXION steel angle and have the same dimensions: $0.55\ m$ long, $0.28\ m$ height, and $0.22\ m$ wide. The baskets are coupled to the arms by a horizontal shaft and two journal bearings $0.0254\ m$ (1") in diameter and separated $0.22\ m$ from each other. The journal bearings operate like a hinge giving the basket a free rotation around a horizontal axis. Its floor and walls are wooden pieces. Three rubber plates located in the center of the basket and fixed to the floor by screws constitute the counterweight. The center of mass of the counterweight is at the same geometrical position as that of the experimental basket. The weight of the basket is approximately $9.8\ kg$. The experimental basket was built with the same materials as the counterweight basket. Its floor is a wooden platform where cuts were made to accommodate the videocamera and the base of the cavity. Inside the experimental basket are located the optical arrangement for flow visualization composed by a laser lamp, a cylindrical prism, a collimating lens, and a cube beamsplitter. All components are located on the same side of the videocamera. As commented before, this arrangement sits on a custom-made support. Detailed description of the design of the visualization system is provided in the following section. Figure 7 shows the spatial distribution of the various parts of the equipment in the experimental basket.

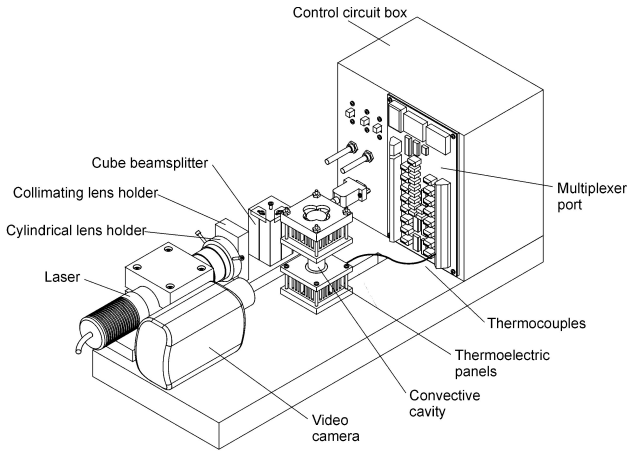

FIGURE 7. Distribution of the elements in the experimental basket.

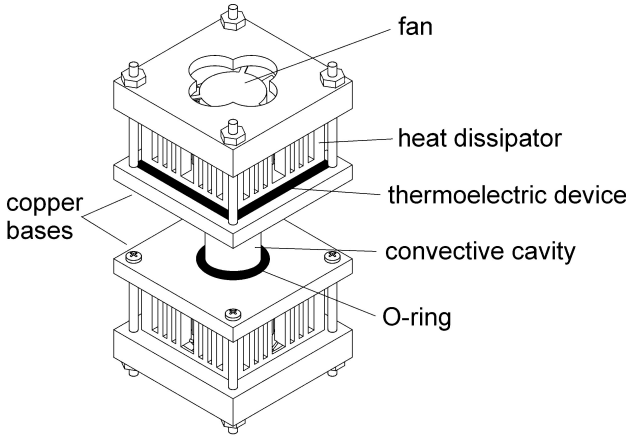

FIGURE 8. Schematic diagram of the cavity.

3.4. Experimental cavity

The experimental basket holds the natural convection cavity and the visualization and control auxiliary equipment. The cavity is located at the center of the basket, seated on the floor. The control circuit and a multiplexer board are located on one side of the cavity and the videocamera on the other. The cavity is constituted of a lateral wall made of a pyrex tube of 17 mm inner diameter with 1.5 mm wall thickness and two flat upper and lower walls made of copper. The ends of the test cell are two copper pieces that house one thermoelectric device each. The temperatures of the ends are controlled to produce the desired axial temperature difference in the cavity. The thermoelectric characteristics are 8 W maximum power consumption at 12 Vdc and operating temperature range of (-79 to 79)$^{\circ}C$. Next to each thermoelectric device and opposite to the cell, a thermal dissipator and a fan are affixed. This heat sink (or source) provides an ambient temperature zone for the thermoelectric devices. The height of the cell is 0.030 m and therefore, its aspect ratio $\Gamma = 1.76$. At a height of 0.0235 m from the bottom and diametrically opposed two small 0.005 m diameter glass tubes are located, through these two thermocouples Omega copper constantan "T" type are positioned to record the temperature of the convective flow. The thermocouples are located at a horizontal distance of 0.003 m from the cavity walls. The schematic diagram of the cavity is shown in Fig. 8.

The voltage of the thermoelectric devices is controlled with a electronic circuit that keeps constant but different temperatures at the top and bottom cavity walls. The electronic circuit is composed of two parts: a) the power circuit and b) the control circuit. The control circuit for one of the thermoelectric devices is shown in Fig. 9. Control is achieved by $U_1(35)$ integrated circuit operating in thermometer mode. This circuit monitors the temperature of the thermoelectric face closer to the horizontal wall of the convective cell continuously and yields an output voltage proportional to the reading with a constant of 10 $mV/^{\circ}C$. An adjustablevoltage divisor constituted by the resistances R_1 and R_3 and the potentiometer R_2 provides the set voltage. The output of thisvoltage divisor is applied to the input of the $U_2(358)$ differential amplifier which is used used as a voltage comparator. Resistances R_4, R_5, R_6, and R_7 together with their corresponding capacitors determine the gain and the response time. The output of this section is called the error signal and is fed into a Darlington power transistor (Q_1) that controls the electric current that goes through the thermoelectric device. The reference voltage is set with a variable resistance and the thermal sensors placed in direct contact with the thermoelectrics provide the input control signal. The control circuit generates the signal to maintain a temperature at the cavity flat wall of rises to $0.47^{\circ}C/s$ and oscillates around the set value with ripples less than $\pm\ 0.5^{\circ}C$.

3.5. On-board CPU and accesories

On the top of the central module of the centrifuge sits a tower that houses the on-board CPU and other instruments. A similar tower is fixed to the ceiling of the room and its lowermost face is separated 0.05 m from the uppermost face of the rotating tower fixed to the central module of the centrifuge. The rotating tower is 1.10 m high and has five shelves. In the first, the laser lamp power supply is located, the second compartment houses the on-board CPU and in the third shelf the hard disk is located. The rest of the space is empty at present in preparation for future use. The on-board CPU is a Pentium II and has one PCLab board. On top of the rotating structure, a circular UHF antenna that is plugged to the video camera output is located. At the end of the fixed structure and separated 0.0254 m (1") from the rotating structure another UHF antenna is placed. This antenna picks up the signal and sends it to the videorecorder and to the monitor to be displayed. The convective motion can be seen in real time.

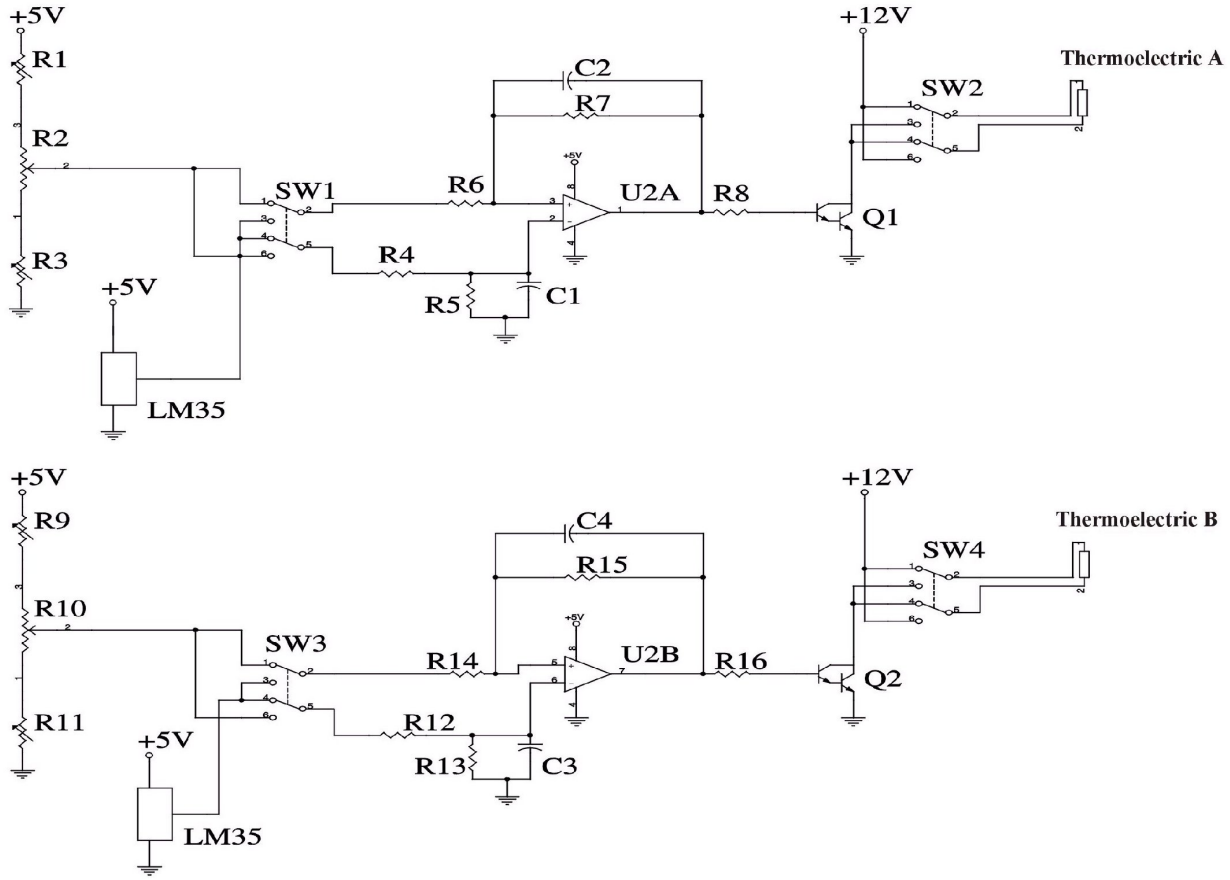

FIGURE 9. Diagram of the control circuit.

3.6. Security fences and bridge

Security fences were built around the centrifuge to protect the laboratory personnel. The fences are constructed with tubular steel tubes. The inner rectangular area formed by the tubular frame, is covered with a stainless steel mesh, $0.01\ m$ ($3/8$ ”). These accessories protect the rest of the area of the laboratory from possible accidents. To reach all of the instruments located at the center of the centrifuge a steel tubular bridge was situated over the centrifuge. Two in-built ladders are located at the bridge feet. The bridge has a loading capacity of more than 100 kg. All of these components are anchored to the floor of the laboratory.

3.7. Foundations

A special foundation platform was constructed to mount the centrifuge on, in order to reduce vibrations caused by other pieces of equipment in the laboratory and also to damp the self-originated vibration due to associated to the rotation of the centrifuge. The foundation area is a rectangular section with the following dimensions 1.5 m^2 and 0.18 m deep. The anti-vibration foundation is constructed with two alternated layers of neoprene, polyfoam and cork. A concrete platform 0.11 *m* deep sits on top of the anti-vibratory sandwich. Finally, on the top of the concrete base, a stainless steel plate is anchored to the concrete. The wiring required to supply power for the motor is embedded in the concrete floor.

4. Instrumentation and sensors

The data acquisition system of the centrifuge is composed of independent arrangements that allow the recording of temperature at various locations of the convective cavity, acceleration at a position close to the cavity, and visualization at the midplane of the test. In this section we describe the instrumentation used to record these variables.

4.1. Temperature

The sensors used for monitoring the temperature are copper-constantan thermocouples (type T thermocouples). These sensors are recommended for measuring temperatures below $100\ ^{\circ}C$. The copper wire diameter is $0.43 \times 10^{-3}\ m$ and the constantan wire diameter is $0.071 \times 10^{-3}\ m$. These sensors are duplex OMEGA [17] teflon insulated fine gage. Two ther-

mocouples are placed in the bottom plate and two in the top plate. One of the thermocouples in the bottom plate is placed in a small hole drilled at the center of the base of the convective cavity. A similar position is occupied by one of the thermocouples in the upper plate. These sensors measure the temperature near the bottom and top of the convective cavity. A thermocouple is located in the bottom plate near the upper face of the thermoelectric device to measured the temperature for control purposes. A similar arrangement is used for the top thermoelectric device.

Temperature readings were captured by an Advantech PCL-818L [18] card with a resolution of 12 bits, linearity of ± 1 bit, and maximum conversion rate of $40\ kHz$. The PCL - 818L uses a PCLD - 789 [19] amplifier/multiplexer board. This board is the front-end signal conditioning and channel multiplexing daugtherboard for the analog input channel. An instrumentation amplifier provides a gain of 200. The multiplexer also contains a cold junction sensing circuit to allow direct measurement of thermocouple transducer $+24.4\ mV/^{\circ}C$ at $0.0\ V$ of $0.0\ ^{\circ}C$. The multiplexer board is fixed close to the electronic control circuit in the experimental basket. We use a flat cable $1.5\ m$ long for connections between the PCLD-789 and PCL-818L, which is inside the on-board CPU fixed on the centrifuge central structure. After an experiment is completed and the centrifuge rotation has stopped, the data are sent via the laboratory network to a mainframe to be permanently stored. A overall view of the centrifuge is shown in the plate 1.

4.2. Acceleration

Another important variable in the centrifuge experimentation is the acceleration. Accelerometers are transducers which transform acceleration into an electrical signal. Variable capacitive accelerometers that measure acceleration signals down to zero hertz use micromachined silicon and variable capacitance elements; these devices have a high sensitivity and minimal response to thermal transients. Specifically, the sensors used are uniaxial K-Beam Kistler accelerometers type 8303A50 [20, 21], with typical sensitivities of approximately $19\ mV/g$ at $30\ Hz$, $3\ g$ rms and a bias voltage of 2.5 *V*. The exact sensitivity varies slightly with the individual device. The transverse sensitivity is approximately 1.0%, its reference range $\pm\ 50g$ peak, and output impedance $\leq 500\ \Omega$.

Three accelerometers are used in the centrifuge. The first one is located in the external module of the centrifuge at a distance of $r = 1.472\ m$ from the axis of rotation. Its orientation is at 90° from the gravitational acceleration vector. This device measures only the centrifugal acceleration $\omega^2 r$. The second device is oriented parallel to **g** and is placed on top of the basket. When the centrifuge is standing still, its horizontal distance to the axis of rotation is $r = 1.445\ m$ and its vertical distance to the basket axis of rotation is $0.0313\ m$. This accelerometer reads the terrestrial acceleration when rotation is zero. At the moment that the centrifuge is operated, the basket will tilt freely and this accelerometer will read a, the resultant acceleration of the vector sum of **g** and the centrifugal acceleration $\omega^2 r\ \mathbf{k}$ where **k** is a unit horizontal vector pointing away from the rotating axis, ω is the rotation velocity, and r is the distance to the rotation axis. The third sensor is vertically aligned with the second accelerometer at a distance $r = 1.445\ m$, from the centrifuge rotation axis and at a vertical separation of $0.228\ m$ from the basket axis of rotation. This accelerometer sits at a position close (and dynamically equivalent) to the convective cavity. When the centrifuge is not rotating, its orientation is horizontal. This device also measures the acceleration a of the convective cavity. The acceleration data are sent from the centrifuge to the laboratory computer using two wireless WaveLan/IEEE Turbo 11 Mb PC Card.

4.3. Data acquisition software

The software package that we used to capture the data was Genie, a data acquisition and control software designed to run in the Microsoft Windows environment. Those system displayed the temperature histories of the two internal thermocouples, the four thermocouples located at the plates and that of the environment temperature. The readings of these seven thermocouples provide convenient, real time information to assess the progress of the experiment.

4.4. Visualization system

The flow visualization is a specialized tool used to better understand complex flow structures. Flow visualization is made using a planar light sheet projected onto a fluid suspension of reflecting particles and viewed at right angles to the plane of illumination. We created a light sheet with a uniform narrow thickness of $0.002\ m$. This illumination was created with an optical arrangement mounted on the experimental basket at the side of the cavity. The visualization system is composed of the following parts: a solid state $50\ mW$ laser lamp, wavelength $\lambda = 543.5\ nm$, a cylindrical prism $0.004\ m$ in diameter, a collimating lens, and a cube beamsplitter ($0.028\ m \times 0.04\ m \times 0.04\ m$). The laser lamp power supply is on-board and is situated on the first shelf of the central structure. The laser lamp is fixed on the platform on the experimental basket with a block base. This platform has three sections. One has a square section base ($0.075\ m \times 0.075\ m \times 0.078\ m$) with a semicircular form in the middle to hold the laser lamp. The second section is a base that supports the collimating lens. The third section is a rectangular base ($0.04\ m \times 0.04\ m \times 0.063\ m$) that holds a cube beamsplitter. All sections are fixed to the platform. A *TR403* Sony CCD videocamera is also housed in the basket to capture the images of the flow in the experimental cavity. The video signal is transmitted to a UHF circular antenna located at the upper part of the central structure. This antenna is separated $0.025\ m$ from the other UHF circular antenna situated on the fixed structure. The signal is transmitted between these two antennas. The fixed antenna is connected to a videorecorder and the signal is sent to an external TV monitor. The visualization system just described allows real time monitoring of the flow in the rotating cavity. The plate 2 shows the experimental basket.

4.5. Particles tracers

The tracers used to visualize the flow inside the cavity are liquid crystal particles. This tracers can be obtained in the form of slurries in water with diameters centered in the range of 10 to 15 μm from Hallcrest [22]. Liquid crystals are organic compounds that exhibit a behavior midway between an isotropic liquid and a nonisotropic crystalline solid. The convenience of using a specific kind of tracers is defined by their capacity of following the flow and of displaying the flow patterns. Although an in-depth analysis of the performance of the tracers can be extremely sophisticated as discussed, for instance, in Ref. 23, the overall performance of the tracers can be easily inferred from the cross validation of the experimental observations with corresponding numerical simulations. Also, we measure the fluid temperature with these liquid crystals in preliminary experiments.

5. Sample results

Once all data and image acquisition systems were working in a satisfactory manner, exploratory runs were performed to test the centrifuge as a unit. From these initial tests we present sample results of the acceleration as a function of time and rotation rate, temperature as function of time, for zero and a constant rotation rate, and two snap–shots of velocity fields as time functions. These results are not to be considered as exhaustive and not even a detailed description of the flow, but just as examples of the kind of scientific information that can be obtained with the device described in this article.

5.1. Acceleration

Using the sensors and auxiliary hardware and software described in Sec. 4.2 and Sec. 4.3, the centrifugal and the total acceleration were measured at three points by the centrifuge. Experimental measurements made with the accelerometer located at the extreme of one arm of the centrifuge yield readings that coincide with the calculated value of $\omega^2 r$ within less than 0.1 m/s^2 in all cases, and in most cases less than 0.04 m/s^2, indicating the consistency between the accelerometer and tachometer readings. Accelerations at the quoted position as a function of time for two rotation rates, ω=1.15 rad/s and ω =2.41 rad/s are shown in Fig. 10. Two kinds of regimes are identified. One where time average acceleration is virtually independent of time and the acceleration displays electronic white noise with amplitude of ± 0.025 m/s^2. This regime exists for $t < 700$ s and 706 $s < t$ in Fig. 10. In the other regime which starts at $t = 720$ s when we change the rotation rate of the centrifuge, and lasts for six seconds, the acceleration displays an approximate linear increase. Given that the response time of the accelerometer is $1/30$ s for the calibration used, it can confidently be asserted that the acceleration readings reflect the inertia of the system.

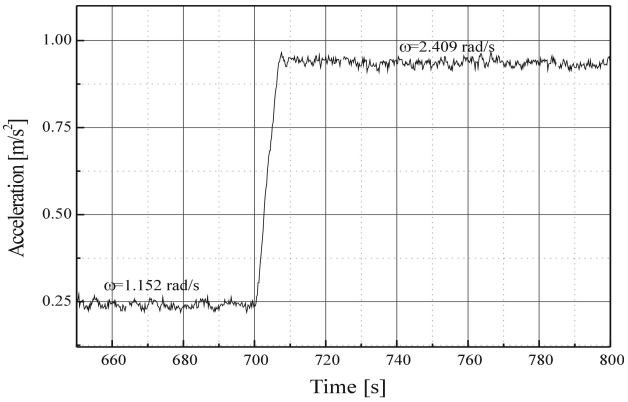

FIGURE 10. Acceleration as a function of time at the extreme of the arm.

The measurements from the accelerometers located in the experimental basket during the constant acceleration periods, which correspond to constant centrifuge rotation velocity, can be calculated using the formula

$$a = \left[g^2 + \left(\omega^2 R \right)^2 \right]^{1/2},$$

where R is the distance from the sensor to the axis of rotation which can be numerically calculated from geometrical considerations as follows:

$$R = r_o + r_1$$

r_o is the length of the arm from the rotation axis to the basket shaft centerline; $r_1 = r_s \cos \alpha$, where r_s is the distance from the basket shaft to the sensor position and $\tan \alpha = g/(\omega^2 R)$. The difference between the experimental records from the two accelerometers in the baskets and the theorical values does not exceed within 13%. The error in the measured acceleration is due to inherent electronic noise, orientation, inexact mounting, and bearing friction in the output reading.

5.2. Temperature and velocity measurements

In this section we present the temperature history as monitored by the internal thermocouples and the velocity fields at specific times. The working fluid is water at room temperature and therefore $Pr = 6$. The aspect ratio is Γ= 1.76 (see the Sec. 3.4). Figure 11 a) shows the temperature recorder by the internal thermocouples, T_1 and T_2 placed in the opposite place site of the cylinder cavity at the same distance from the bottom. In the first stage, there is not axial temperature difference in the cell ($Ra = 0$) and the centrifuge does not rotate ($Ta = 0$). At $t = 300$ s the second stage begins, the lower thermoelectric turned on to produce the axial temperature difference in the cavity of 0.158 $^\circ C/mm$, ($Ra = 2.25 \times 10^6$) and the centrifuge continues in stationary mode ($Ta = 0$). The third stage at $t = 1800$ s when the centrifuge is set in rotation with angular velocity of $\omega = 2.33$ rad/s (22 rpm) with $Ta = 1.71 \times 10^7$ having a $Ra_r = 3.25 \times 10^6$. The final stages begins at $t = 2700$ s when the centrifuge stops rotation having a $Ra = 2.06 \times 10^6$.

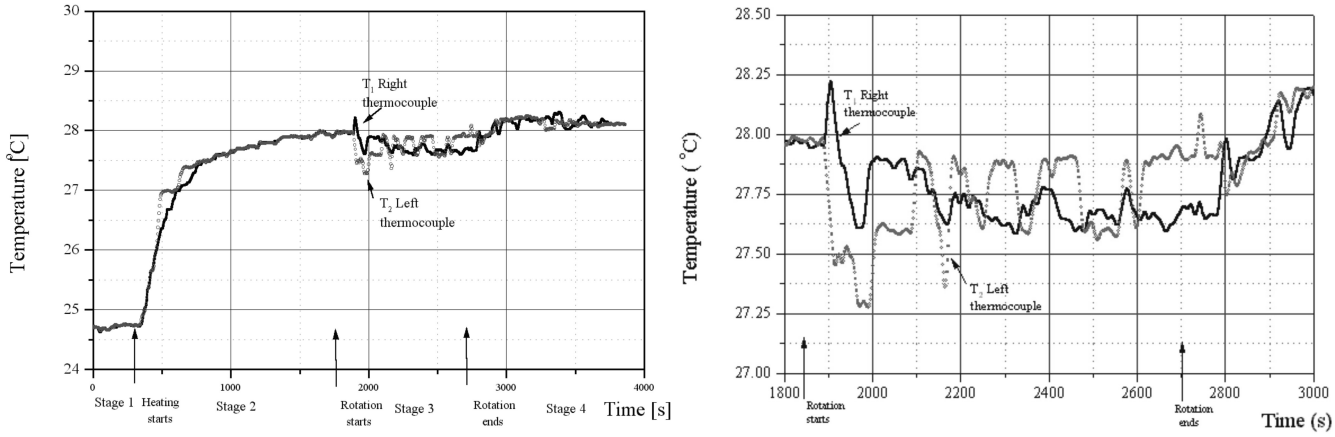

FIGURE 11. Temperature as a function of time a) during a sample experiment with four different stages. and b) amplification of the stage 3, $Ra_r = 3.25 \times 10^6$, $Pr = 6$, and $Ta = 1.71 \times 10^7$.

In the first stage the temperatures are almost constant. In the second stage the temperatures increase monotonically during the first $1300\ s$ before attaining an almost constant temperature. A small temperature difference exists between the two thermocouples in the second stage. When the rotation begins the temperatures display a dramatic change in qualitative behavior. The temperature oscillates at a frecuency of about 0.0033 Hz (see the amplification in Fig. 11.b). In the fourth stage, when rotation stops, the oscillation of the temperatures is damped, attaining a similar behavior of the one before onset of rotation [24]. Figures 12 a) and 12 b) show the mean velocity fields in the central plane of the cavity for two different states. In the upper left hand corners, we note a zone without vectors due to the thermocouples mounting system. Each mean velocity field in the average of 449 velocity fields of each velocity field is obtained from a cross correlation, made with the Flow Manager PIV software of Dantec, of a pair of images taken at time intervals of 0.033 s. In the Fig. 12 a) we can observe a single convective cell rotating in the counterclockwise direction. This pattern is obtained during the second stage, when $Ra = 2.25 \times 10^6$ and $Ta = 0$. The center of the convective cell is not positioned at the center of the cavity. At 0.65 of the cavity height a strong vertical movement occurs at the right side. The velocity field shown in Fig. 12 b corresponds to the rotation stage (third stage) with $Ra = 3.25 \times 10^6$ and $Ta = 1.71 \times 10^7$. The flow pattern displays a marked difference from the non-rotation pattern (Fig. 12 a). In the middle section of the cavity a general downward movement is observed. One can also note a diagonal movement in the center of the cavity. A comprehensive description of the flow without and with rotation, will be given in a future publication.

6. Concluding remarks

We have designed and constructed a low cost centrifuge. The instrumentation is versatile and can perform a variety of fluid dynamic experiments in a rotating frame of reference. The rotating velocity and arm length can be changed easily allowing a reasonably wide range of experimental conditions. The highest centrifugal acceleration is approximately $13\ g$. Using the centrifuge in its present configuration, we have been able to record temperature, acceleration, and images of particle tracers that contain information of the two dimensional velocity field. Future uses of the centrifuge could include crystal growth and material deposits with chemical baths, combustion and others.

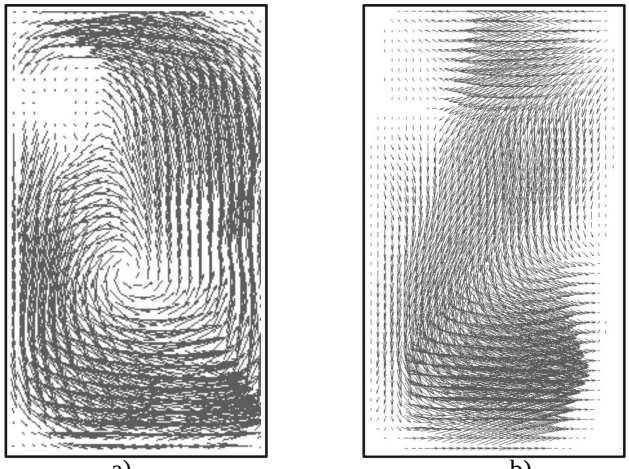

a) b)

FIGURE 12. Convective flows a) in the nonrotating cavity, $Ra = 2.25 \times 10^6$, $\mathrm{Pr} = 6$, $Ta = 0$ and $t = 1380\ s$. and b) in rotating cavity, $Ra_r = 3.25 \times 10^6$, $\mathrm{Pr} = 6$, $Ta = 1.71 \times 10^7$ and $t = 1920\ s$.

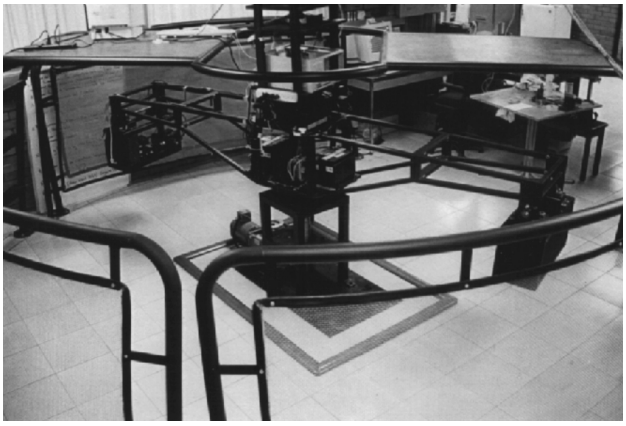

PLATE 1. Overall view of the centrifuge.

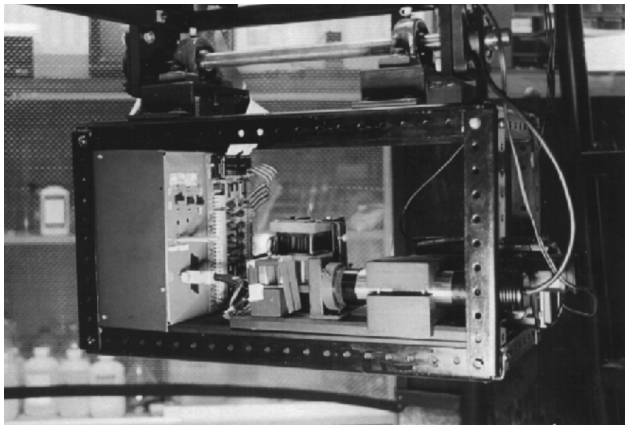

PLATE 2. Experimental basket.

Acknowledgments

Most of the centrifuge was built at Centro de Ciencias Aplicadas y Desarrollo Tecnológico, CIADET–UNAM. We wish to thank the assistance of Leopoldo Ruíz, Alberto Caballero and Juan Arenas from CIADET-UNAM. The Engineering drawings were done by Luis Velázquez from CIADET-UNAM. Hector Perales from FC-UAEMor assisted in computer and visualization tasks. We thank Guadalupe Huelsz for her crucial aid in PIV technique. Fernando Sierra from CIE-UNAM participated in the performance of the experimental runs and in the interpretation of results. A.A. Avramenko also participated in the analysis of experimental observations and also to Hugo Salas for his comments in the organization of the article. The financial support through CONACYT Group Project G0044E financial support is gratefully acknowledged.

1. B. V. Burdin, L. L. Regel, A. M. Turtchaninov, and O.V. Shumaev, *J. Cryst. Growth.* **119** (1992) 61.
2. R. Rodot, L. L. Regel and H. M. Turtchaninov, *J. Cryst. Growth*. **104** (1990) 280.
3. M. J. Paulin *et al*. in *Materials Processing in High Gravity*, edited by L. L. Regel and W. R. Wilcox, (Plenum Press, New York 1994), p. 213.
4. T. Hibiya, S. Nakamura, K. W. Yi and K. Kukimoto in: L. L. Regel, W. R. Wilcox (Eds), *Material Processing in High Gravity*, Plenum Press, New York (1994) 170.
5. R. Derebail, W. A. Arnold, G. J. Rosen, W. R. Wilcox and L. L. Regel in: L. L. Regel, W. R. Wilcox (Eds), *Material Processing in High gravity*, Plenum Press, New York (1994) 203.
6. G. Müller and G. Neumann, *J. Cryst. Growth*. **59** (1982) 548.
7. G. Müller, G. Neumann and W. Weber, *J. Cryst. Growth*. **119** (1992) 8.
8. W. Weber, G. Neumann, and G. Müller, *J. Cryst. Growth.* **100** (1990) 145.
9. L. L. Regel and W. R. Wilcox, *Materials Processing in High Gravity*, Plenum Press, New York (1994).
10. L. L. Regel and W. R. Wilcox, *Centrifugal Material Processing*, Plenum Press, New York (1997).
11. L. L. Regel and W. R. Wilcox, *Processing by Centrifugation*, Plenum Press, New York (2001).
12. S. Chandrasekhar, *Hydrodynamic and Hidromagnetic Stability.* Dover. (1961).
13. B. M. Boubnov and G. S. Golitsyn, *Convection in Rotating Fluids*. Kluwer London. (1994).
14. G. Müller, G. Neumann and W. Weber, *J. Cryst. Growth*. **70** (1984) 78.
15. L. M. de la Cruz. Natural convection in a rotating cavity, B Sc. Physics Thesis UNAM (In spanish) (1996).
16. Yaskawa Electric Corp, *VS miniC Series ultra compact all digital inverter*. (1995).
17. Omega, *The Temperature Handbook*, 1998.
18. Advantech PCL-818L High performance low cost. Data Acquisition Card. User Manual PC-lab Card. (1995).
19. Advantech, *PCLD-789 Amplifier/Multiplexer Board User's manual*. (1992).
20. Kistler, *Advanced instrumentation for a world of applications*. (1998).
21. Kistler, *Operation Instructions K Beam capacitive accelerometers.* 1998.
22. Hallcrest, *The Hallcrest Handbook of Thermochoromic Liquid Crystal Technology*, England (1996).
23. J. C. Agüi and J. Jimenez, *J. Fluid Mech.* **185** (1987) 447.
24. M. Vargas, E. Ramos, F. Sierra and A. Avramenko in: L. L. Regel, W. R. Wilcox (Eds). Processing by Centrifugation, Plenum Press, New York (2001).